CMLS, Cell. Mol. Life Sci. 60 (2003) 2189–2199
1420-682X/03/102189-11
DOI 10.1007/s00018-003-3187-4

CMLS Cellular and Molecular Life Sciences

Research Article

HCN channels contribute to the intrinsic activity of cochlear pyramidal cells

B. Pál[a], Á. Pór[a], G. Szűcs[a], I. Kovács[b] and Z. Rusznák[a,*]

[a] Department of Physiology, Medical and Health Science Centre, University of Debrecen, PO Box 22, 4012 Debrecen (Hungary), Fax: +36 52 432 289, e-mail: rz@phys.dote.hu
[b] Department of Pathology, HBM Kenézy Gyula County Infirmary, Bartók Béla u. 2-26, 4043 (Hungary)

Received 15 May 2003; received after revision 26 June 2003; accepted 21 July 2003

Abstract. A hyperpolarization-activated current recorded from the pyramidal cells of the dorsal cochlear nucleus was investigated in the present study by using 150- to 200-µm-thick brain slices prepared from 6- to 14-day-old Wistar rats. The pyramidal neurones exhibited a slowly activating inward current on hyperpolarization. The reversal potential of this component was –32 ± 3 mV (mean ± SE, n = 6), while its half-activation voltage was –99 ± 1 mV with a slope factor of 10.9 ± 0.4 mV (n = 27). This current was highly sensitive to the extracellular application of both 1 mM Cs^+ and 10 µM ZD7288. The electrophysiological properties and the pharmacological sensitivity of this current indicated that it corresponded to a hyperpolarization-activated non-specific cationic current (I_h). Our experiments showed that there was a correlation between the availability of the h-current and the spontaneous activity of the pyramidal cells, suggesting that this conductance acts as a pacemaker current in these neurones. Immunocytochemical experiments were also conducted on freshly isolated pyramidal cells to demonstrate the possible subunit composition of the channels responsible for the genesis of the pyramidal h-current. These investigations indicated the presence of HCN1, HCN2 and HCN4 subunits in the pyramidal cells.

Key words. Cochlear nucleus; pyramidal cell; I_h; spontaneous activity; HCN subunits.

The pyramidal (or fusiform) cells form one of the prominent cell types of the dorsal cochlear nucleus. These neurones have a triangular cell body approximately 25 µm in diameter [1], from which basal and apical dendritic trees extend [2–4]. The apical dendritic tree reaches the molecular layer of the nucleus, and makes several contacts with the glutamatergic parallel fibre network provided by the cochlear granule cells. The basal dendrites, on the other hand, are contacted with primary acoustic nerve fibres, also forming glutamatergic synapses. The axons of the pyramidal neurones are understood to enter the dorsal acoustic stria and eventually project to the contralateral inferior colliculus [5, 6].

A previous study demonstrated that the resting membrane potential of the pyramidal cells is between –50 and –60 mV [7]. These neurones produce spontaneous activity, whose mechanism and genesis are not yet clearly understood. Some of the membrane properties of the pyramidal cells, however, have been extensively studied. The pyramidal cells are commonly accepted to produce several distinct firing patterns in response to incoming stimuli (generally known as 'pauser', 'chopper' and 'buildup' firing characteristics [3, 8]), and the availability of a rapidly inactivating A-type K^+ current has been shown to have essential roles in determining the type of response pattern observed after stimulation [9]. In addition to the rapidly inactivating current, however, a more slowly inactivating, tetraethyl-ammonium $(TEA)^+$-and 4-aminopyridine (4-AP)-sensitive component has also been described

* Corresponding author.

[9]. Besides these transient current components, pyramidal cells possess a persistent Na^+ current as well [10], which becomes activated near to the resting membrane potential.

Pyramidal cells also express several depolarization-activated Ca^{2+} channels [11]. In fact, every known type of Ca^{2+} current has been identified in the membrane of the fusiform neurones, and the presence of some of the Ca^{2+} channel components was confirmed using immunocytochemistry [11]. Activation of $GABA_B$ receptors could reversibly depress the amplitude of the N-type Ca^{2+} current, indicating that GABA-ergic inputs to the pyramidal cells may be involved in determining the membrane properties of these neurones.

Despite recent advances in describing the major membrane currents of the pyramidal cells, the previously conducted studies somehow ignored the possible contribution of the hyperpolarization-activated conductances to the overall membrane properties of the pyramidal cells. This seems surprising, especially if one considers that the possible source of the spontaneous activity of the pyramidal cells might be a hyperpolarization-activated non-specific cationic current, as indicated in some other structures with pacemaker activity (e.g. heart and neurones) [12–16]. We therefore decided, to seek evidence for the presence of this kind of current on the pyramidal cells, and to investigate whether this conductance (if present) is involved in their spontaneous activity.

Our results show that pyramidal cells express a hyperpolarization-activated non-specific cationic conductance recognised as I_h. Immunocytochemical techniques demonstrated that HCN1, HCN2 and HCN4 subunits were present in the membrane of the pyramidal cells. This study also shows that the activity of the spontaneously active pyramidal cells was substantially reduced when I_h was inhibited (by the extracellular application of either CsCl or the more specific ZD7288), suggesting that this non-specific cationic conductance makes a major contribution to the genesis of the spontaneous firing.

Materials and methods

Preparation of dorsal cochlear nuclear slices

The basic steps of the preparation were similar to those described earlier [17], but the method had to be adapted to the slicing of the dorsal cochlear nucleus. Briefly, brain slices were prepared from 6- to 14-day-old Wistar rats, killed by decapitation. The brain was then transferred into ice-cold (~–2 °C) low-sodium artificial cerebrospinal fluid (aCSF). The meninges and blood vessels were carefully removed, and the brain was bisected along the midline. After removal of the cerebral hemispheres, both brain halves were glued to a Teflon block with cyanoacrylate glue. The cerebellum was removed from both tissue pieces, and a 600-µm-thick slice was cut to remove the ventral part of the cochlear nucleus. After discarding the ventral cochlear nucleus, three to five 150- to 200-µm-thick slices were prepared from the dorsal cochlear nucleus, which contained the pyramidal cells. The slicing was carried out employing a Campden vibratome (Campden Instruments, Loughborough, UK). The slices were then transferred to an incubation chamber containing normal aCSF, preheated to 37 °C, and bubbled with 95% O_2/5% CO_2. The slices were maintained in this solution for 1 h and were then allowed to cool to room temperature (~20–22 °C).

The composition of the normal aCSF was (mM): NaCl, 125; KCl, 2.5; $NaHCO_3$, 26; glucose, 10; NaH_2PO_4, 1.25; $NaHCO_3$, 26; $CaCl_2$, 2; $MgCl_2$, 1; myo-inositol, 3; ascorbic acid, 0.5; sodium pyruvate, 2. In the low-sodium aCSF, NaCl was replaced by sucrose. The pH of both solutions was 7.2 when gassed with 95% O_2/5% CO_2, the osmolarity of the solutions was 310 mosm/l. All chemicals were purchased from Sigma (St. Louis, Mo.), unless stated otherwise.

Data recording

The slices were placed into an environmental chamber (~200 µl) and continuously perfused (~1 ml/min) with gassed aCSF solution, using an eight-channel Minipulse 3 peristaltic pump (Gilson, Villiers Le Bel, France). When the spontaneous activity of the cells was to be inhibited, the extracellular solution contained 1 µM tetrodotoxin (TTX; Alomone Labs, Jerusalem, Israel). For some of the measurements, various K^+ channel blockers (1 mM TEA^+, 2 mM 4-AP), CsCl and ZD7288 (a kind gift from Dr. I.D. Forsythe) were also applied, by switching perfusion between the available channels of the peristaltic pump.

Whole-cell patch-clamp pipettes were fabricated from thin-walled borosilicate glass (Clark Electromedical Instruments, Reading, UK), and filled with a solution containing (mM): KCl, 130; HEPES, 10; $MgCl_2$, 1; EGTA, 5; MgATP 2; Na_3-GTP 0.5; pH 7.3; osmolarity set to 300 mosm/l. The resistance of these patch-pipettes varied between 2 and 2.5 MΩ when filled with the pipette solution. Cells with large, triangular cell bodies were selected for this study. These neurones were patch-clamped under visual guidance, without prior cleaning. The series resistance was usually between 2–8 MΩ and was compensated by 60–80%. The series resistance was kept as constant as possible during the measurements, by occasional light suction or repositioning of the pipettes. Both the voltage- and current-clamp configurations of the patch-clamp technique were employed. An Axopatch 200A patch-clamp amplifier was used for recording, together with a DigiData 1200 interface (Axon Instruments, Foster City, Calif.). For data acquisition and analysis, the pClamp 6.0 software was used. The whole-cell capaci-

tance was electronically compensated. Results are given as means ± SE.

Differential interference contrast microscopy

The recording chamber was mounted on an Axioskop fixed-stage microscope (Zeiss, Oberkochen, Germany), equipped with Nomarski optics (differential interference contrast; DIC) and an epifluorescent attachment. A Zeiss Achroplan water immersion objective was used (×63) for cell visualization. Cell identity was confirmed by including Lucifer Yellow (dipotassium salt, 0.5 mg/ml) in the pipette solution and by switching to the epifluorescent illumination of the experimental microscope after the recordings. As the pipette solution contained Lucifer Yellow, the light of the microscope was switched off prior to entering the whole-cell configuration.

Enzymatic isolation of dorsal cochlear nuclear pyramidal neurones

Dorsal cochlear nuclear neurones were isolated using a technique described earlier in detail [18]. In brief, 3- to 8-day-old rats were decapitated, their brain removed in low Na^+ aCSF, and the dorsal cochlear nuclei incubated in aCSF containing 0.03 mg/ml collagenase (type IA) and 0.12 mg/ml pronase (type XIV) for 40 min at 31 °C. During the enzyme treatment, the incubating solution was bubbled with 95% O_2/5% CO_2 throughout. The enzyme exposure was terminated by the application of trypsin-inhibitor (type I-S, 1 mg/ml). At the end of the isolation procedure, the cells were dispersed using gentle mechanical trituration in HEPES-buffered aCSF (in mM: NaCl, 135; KCl, 3; glucose, 10; HEPES, 10; sucrose, 30; $CaCl_2$, 2; $MgCl_2$, 1; osmolarity and pH were set to 335 mosmol/l and 7.2, respectively).

Immunocytochemistry

Immunocytochemical labelling was performed on acutely isolated dorsal cochlear nuclear neurones. After enzymatic dissociation, the cells were fixed with concentrated (99%) acetone (5 min at 4 °C). Aspecific binding was prevented and permeabilization was carried out by bathing the cells in phosphate-buffered saline (PBS) containing bovine serum albumin (BSA, 1%) and Triton X-100 (0.6%) for 30 min. The cells were then incubated with the primary antibody [rabbit anti-HCN1, 2 or 4 (1:200); Alomone Labs.] for 60 min at room temperature. The cells were rinsed in PBS (3 × 5 min), incubated with goat anti-rabbit FITC-conjugated or horse anti-rabbit Texas-Red-conjugated secondary antibodies (1:400) for 60 min at room temperature, followed by rinsing in PBS again (3 × 5 min). Neurone-specific immunoreaction was carried out using anti-neurone-specific enolase (mouse anti-NSE; 1:100) antibodies, and horse anti-mouse FITC- or Texas-Red-conjugated secondary antibodies (1:400). At the end of the procedure, the nuclei were stained with DAPI followed by coverslip mounting.

In the other set of experiments, the acutely isolated cells were allowed to adhere to adhesive-coated (3-aminopropyltrethoxysilane) coverslips for 20 min, and were then washed with PBS. The cells were fixed with 96% ethanol (10 min at 4 °C), followed by antigen retrieval in a pressure cooker (lasting for 2 min). In the cases of the HCN1 and HCN2 immunolabelling, antigen retrieval was performed in 0.01 M citrate buffer (pH = 6.0), while the HCN4 antigen exposure was carried out in 0.001 M Tris-HCI buffer (pH = 8.8). Inhibition of the endogenous peroxidase was achieved using 3% H_2O_2 solution for 10 min at room temperature. Aspecific binding was prevented by incubating the cells in Tris-buffered saline (TBS) containing 1% BSA (1 h at room temperature). The primary antibodies (both the anti-HCN and NSE; DAKO, Glostrup, Denmark) were dissolved in 1% BSA, and the cells were bathed in these solutions at room temperature for 1 h (anti-HCN1 and anti-HCN-2 1:20; anti-HCN4 1:10; anti-NSE 1:200). The cells were then rinsed in TBS (3 × 5 min) and the secondary antibodies were applied (biotinylated goat anti-rabbit and anti-mouse IgG 1:100) for 30 min, and rinsed again in TBS (3 × 5 min). The immunoreactions were then visualized using diamino-benzidine (DAB) and Fast Blue. At the end of the procedure, the cells were washed with distilled water and mounted onto a coverslip.

When the immunolabelling was finished, the cells were viewed employing a Nikon Axiovert 600 microscope equipped with a ×200 objective.

Results

To ensure that only pyramidal cells were investigated in the present study, cells with large (up to 20 µm in diameter), triangular cell bodies were selected in the brain slices. As the pipette solution always contained Lucifer Yellow, the shape of the soma could be confirmed and the morphology of the dendritic tree could also be assessed (fig. 1A–E). Figure 1E demonstrates the image of a cell identified as a pyramidal neurone. In general, pyramidal neurones had triangular cell bodies which gave rise to three major processes, corresponding to the apical and basal dendrites and to the axon. Cells without these morphological features were omitted from the subsequent data analysis.

As shown in figure 2A, when the pyramidal cells were subjected to hyperpolarizing stimuli from a holding potential of –60 mV, they produced a slowly activating inward current. The current had an instantaneous component, which became obvious after the decay of the capacitive transient. The current showed slow activation and demonstrated no inactivation during the 2-s-long (or in

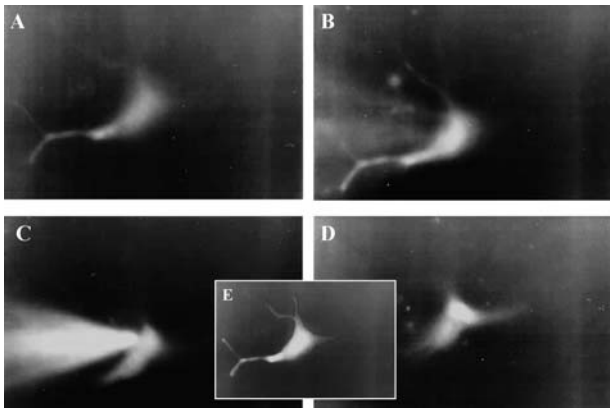

Figure 1. A pyramidal cell in a brain slice prepared from the dorsal cochlear nucleus. The images were recorded using a Zeiss Axioskop FS equipped with epifluorescent illumination and a ×63 water-immersion objective. (*A–D*) The same cell, whose image was taken at various optical depths (*A*, deepest layer; *D* most superficial one). Besides the various parts of the cell, the microelectrode used for the filling and electrophysiological recording is also visible in *B*, *C*. (*E*) Merge of *A–D*.

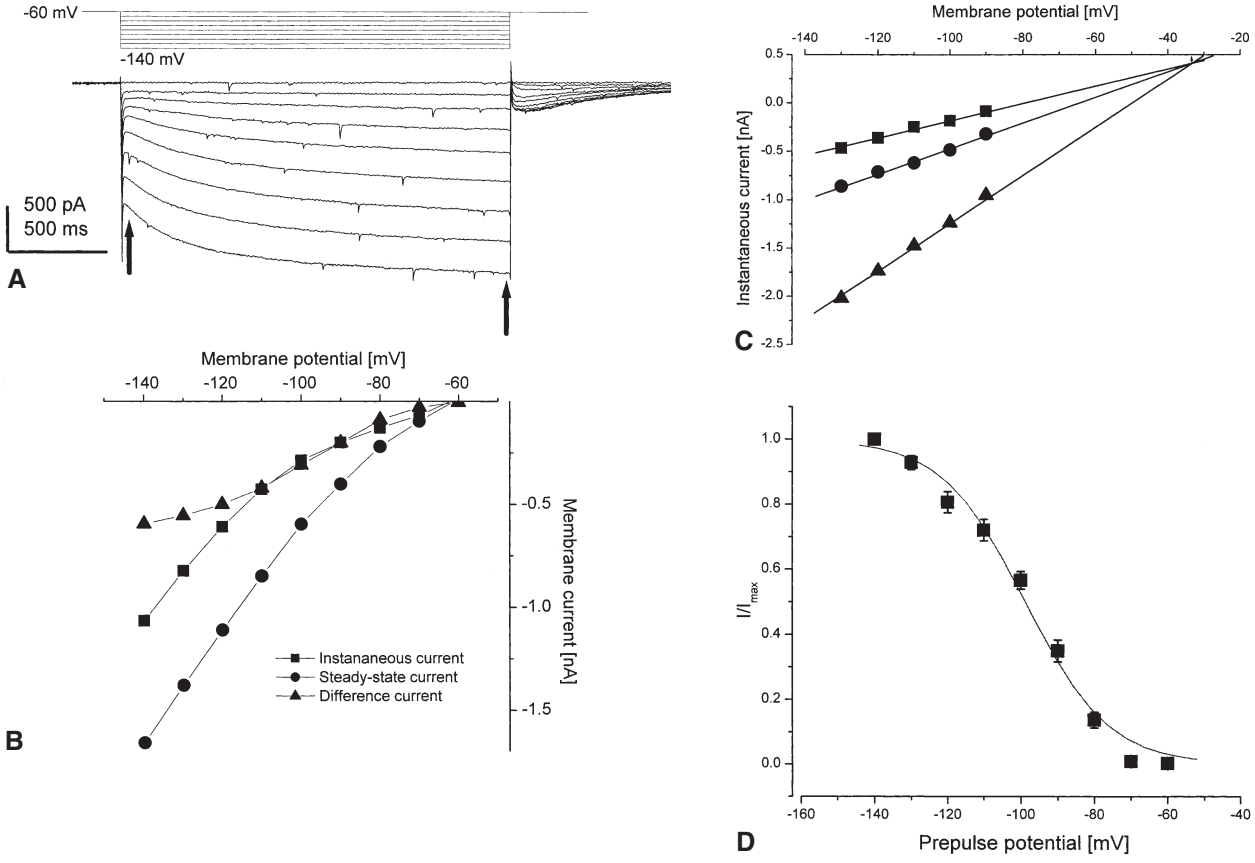

Figure 2. General characteristics of the hyperpolarization-activated current recorded from cochlear pyramidal cells. (*A*) The current recorded under voltage-clamp conditions when 2-s-long hyperpolarizing stimuli were applied from a holding potential of –60 mV. Arrows demonstrate the times when the instantaneous and steady-state current amplitudes were determined. (*B*) The instantaneous (squares) and steady-state (circles) current amplitudes as a function of the membrane potential. The voltage-dependence of the difference current (obtained by subtracting the instantaneous current amplitude from the steady-state current; triangles) is also presented. (*C*) The reversal potential of the hyperpolarization activated current was determined by determining the instantaneous current amplitudes from holding potentials of –60 mV (squares), –70 mV (circles) and –80 mV (triangles) and plotting them as a function of the membrane potential. The intersection point gives the reversal potential of the current (for further explanation see Results). (*D*) The steady-state activation characteristics of the hyperpolarization-activated current. In these experiments, hyperpolarizing voltage steps were employed from a holding potential of –60 mV in 10-mV increments. After each hyperpolarizing step, the amplitude of the tail current was determined, and the individual values were normalized to the tail current amplitude observed after the –140-mV hyperpolarization. The normalized current values (mean ± SE) are plotted against the membrane potential of the preceding hyperpolarizing voltage steps, and the individual data fitted to a Boltzmann distribution (fitted curve).

some instances during the 15-s-long) hyperpolarizing stimuli. When the membrane potential was switched back to the holding potential, the current produced an inward tail component. The current-voltage relationship of both the instantaneous (measured just after the capacitive transient) and the steady-state current were determined as shown in figure 2B.

The slow activation, the lack of the inactivation tendency, along with the inward tail current occurring at the holding potential (–60 mV) suggested that the current observed here possibly corresponded to a non-specific cationic conductance known as I_h. As the h-current is a mixed cationic current, its reversal potential is expected to be around –30 mV. However, at this membrane potential, several depolarization-activated K^+ and Ca^{2+} currents may interfere with the determination of the reversal potential if a tail-current protocol is employed. For this reason, a different method was used in this work, where the reversal potential of I_h was sought by determining the instantaneous current voltage relationship between –90 and –130 mV from three different holding potentials (–60, –70 and –80 mV), and the intersection points were then determined as shown in figure 2C. The intersection point provided the equilibrium potential of this mixed cationic current, which proved to be –32 ± 3 mV (n = 6).

The steady-state activation parameters of I_h are known to show a certain degree of variation depending on the type of neurone investigated. The half-activation voltage (E_{50}) of the I_h expressed by neurones of the auditory apparatus are usually more negative than the E_{50} reported for other types of neurones, hence we deemed interesting an investigation of whether the pyramidal cells of the dorsal cochlear nucleus fit into this trend (fig. 2D).

The steady-state activation of the h-current was investigated using a tail-current protocol. First, 2000-ms-long prepulses were applied between –70 and –140 mV from a holding potential of –60 mV, and the tail-current amplitudes were determined at –60 mV. These current amplitudes were then normalized to the maximum tail-current amplitude, which was measured after the application of the most negative prepulse potential (to –140 mV). The normalized tail current amplitudes were plotted against the prepulse potential and the resulting values gave a sigmoid curve, which was fitted to a Boltzmann distribution of the following form:

$$I/I_{max} = \left\{1 + \exp\left[\frac{E_{50} - E}{s}\right]\right\}^{-1}, \quad (1)$$

where I is the current evoked after the prepulse potential E, I_{max} is the maximal current, E_{50} is the prepulse potential at which half of the channels are activated, while s is the slope factor.

In the cases of the pyramidal cells of the dorsal cochlear nucleus, the half activation voltage was –99 ± 1 with a slope factor of 10.9 ± 0.4 (n = 27).

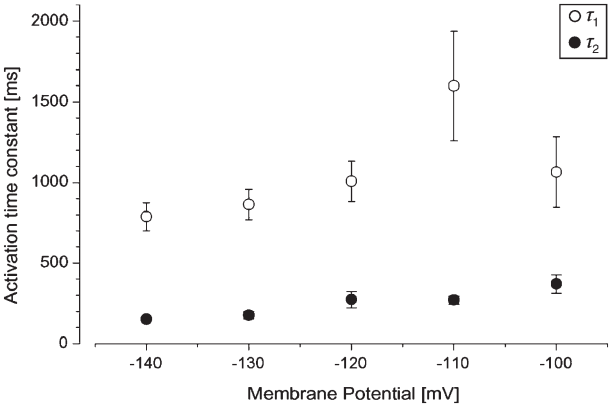

Figure 3. Voltage dependence of the activation time constants of the hyperpolarization-activated current. In these experiments, current traces were evoked from a holding potential of –60 mV to the membrane potential indicated in the figure. The capacitive transient of the current traces was omitted from the analysis, and the remaining current was fitted to a double exponential function. The data plotted in the diagram show the mean values (± SE) of both the faster (τ_1; filled circles) and slower (τ_2; open circles) activation time constants.

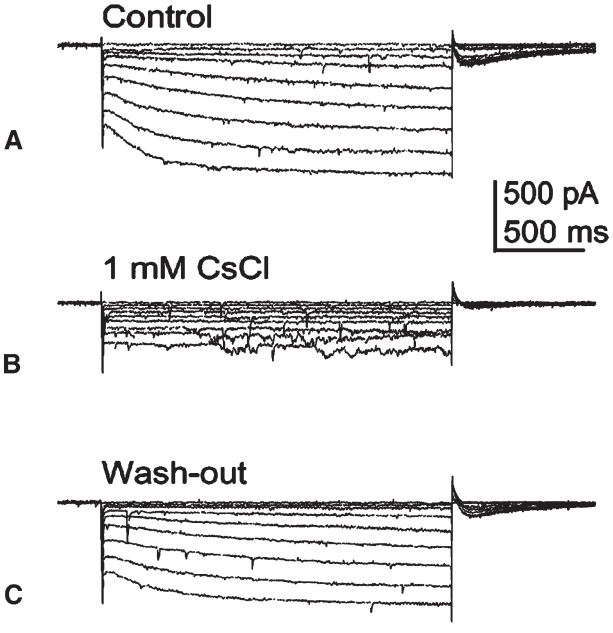

Figure 4. Effect of extracellular CsCl on the hyperpolarization-activated current. (*A*) The current traces were evoked by applying 2-s-long hyperpolarizing stimuli from a holding potential of –60 mV. The hyperpolarizing steps followed each other in 10-mV increments to a maximum hyperpolarization of –140 mV. (*B*) After recording the control current, 1 mM CsCl was employed in the extracellular solution and the same voltage protocol repeated. (*C*) The current which could be recorded from the same neurone after a 9-min wash-out period.

To describe the kinetic properties of the I_h activation, the activation time constants were determined by fitting the current traces to an appropriate exponential function. Traces recorded between –140 and –100 mV were fitted only, as at less negative membrane potentials the fitting became unreliable. Both single and double exponential functions were tried to achieve proper fits, and the application of the double exponential function resulted in more reliable results. Figure 3 demonstrates the voltage dependence of both time constants. The relative contribution of the two components to the total current was approximately 50% at all membrane potentials tested.

The hyperpolarization-activated cationic current is known to be sensitive to the extracellular application of CsCl, which was the case in the cochlear pyramidal cells as well (fig. 4). First, the current traces were evoked in the control extracellular solution, by using the same voltage protocol introduced in conjunction with figure 2A, then 1 mM CsCl was applied in the bath solution, and the same pulse protocol was repeated. As can be seen, this manoeuvre almost completely abolished the slowly activating inward current. It is also demonstrated that the effect of Cs^+ could be reversed to a certain extent. Considering all the cells tested, 1 mM CsCl reduced the hyperpolarization-activated current amplitude (which was calculated by subtracting the instantaneous current from the steady-state current) by 85 ± 9% (n = 12; –140 mV). In some of experiments, the Cs^+ concentration was increased to 5 mM and the blocking effect was similar to that found in the presence of 1 mM CsCl (87 ± 7%, n = 5).

During the experiments, a certain portion of the pyramidal cells showed spontaneous activity (69 cells out of 98). Such activity is demonstrated in figure 5A, and we decided to assess whether the h-current in the pyramidal neurones made any contribution to the spontaneous activity recorded. To reveal the significance of the h-current in the genesis of the spontaneous activity, first the intrinsic activity of the neurones was determined in control extracellular solution, then the procedure was repeated in the presence of 1–5 mM CsCl (fig. 5B; 5 mM CsCl). As demonstrated (particularly in fig. 5C), the slow depolarization, which preceded the action potential firing, became shallower, and thus the frequency of the spontaneous firing decreased, although it was not eliminated entirely. Similar experiments were repeated on four more neurones, with the same result. A summary of these experiments is indicated in figure 5D. To construct this figure, the spontaneous firing frequency was measured in control solution first, then in the presence of 1–5 mM CsCl. Note that the columns represent normalized frequencies, which were calculated by dividing the firing

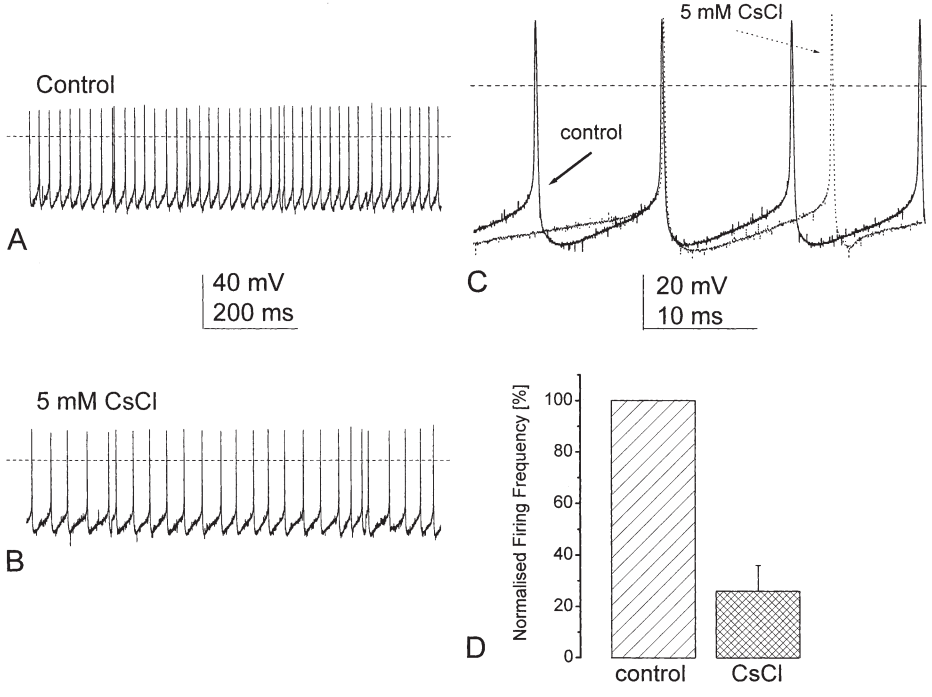

Figure 5. Effect of extracellular CsCl on the spontaneous activity of the pyramidal cells. (*A, B*) Spontaneous action potential firing of a pyramidal cell under control conditions (*A*) and in the presence of 5 mM CsCl (*B*). In these experiments the whole-cell configuration was established, the membrane potential was recorded, but no stimulation was applied to the cell. (*C*) The time scale was changed and the control and Cs^+-affected firings were overlapped to compare the two situations. (*D*) Synopsis of all data recorded under similar circumstances. The frequency of the spontaneous action potential produced in the presence of CsCl was normalized to the control activity in each cell, and the mean value (± SE) of these normalized frequencies is shown.

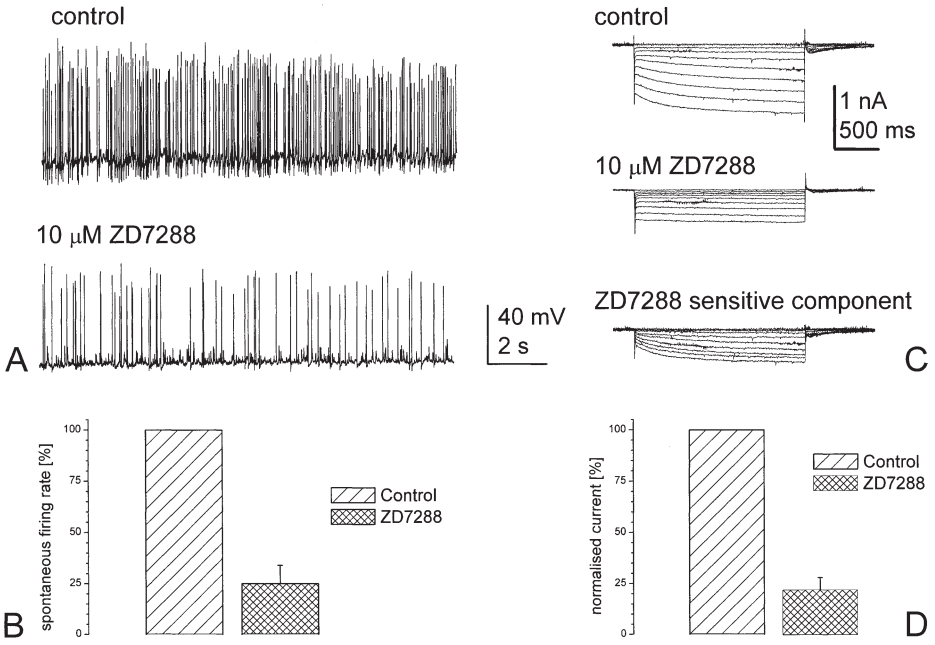

Figure 6. Effect of the h-current-specific blocker, ZD7288, on the hyperpolarization-activated current and spontaneous activity of the pyramidal cells. (*A*) The spontaneous activity of a pyramidal cell under control conditions and in the presence of 10 μM ZD7288. (*B*) Synopsis of all experiments conducted in a similar way. The frequency of the spontaneous action potential produced in the presence of ZD7288 was normalized to the control activity in each cell, and the mean value (± SE) of these normalized frequencies in this part of the figure. (*C*) The effect of ZD7288 on the hyperpolarization-activated current produced by a pyramidal cell. In this (and similar) experiment(s), the current traces were evoked by applying 2-s-long hyperpolarizing stimuli from a holding potential of –60 mV. The hyperpolarizing steps followed each other in 10-mV increments to a maximum hyperpolarization of –140 mV. After recording the control current, 10 μM ZD7288 was employed in the extracellular solution and the same voltage protocol repeated. The third set of traces presents the drug-sensitive current. The traces were obtained by subtracting the current traces yielded in the presence of ZD7288 from those recorded under control conditions. (*D*) The result of all similar experiments. The current amplitude (defined as the steady-state current minus the instantaneous component measured at –140 mV) recorded in the presence of ZD7288 was normalized to that obtained in control extracellular solution (mean ± SE).

rate in the presence of the blocker with that recorded under control circumstances. Considering all the cells tested, CsCl reduced the intrinsic activity to 26 ± 10% of the control situation (n = 5). These results suggested that the h-current was indeed involved in the genesis of the spontaneous activity of the pyramidal cells, acting as a pacemaker conductance.

CsCl is not specific to I_h but is capable of inhibiting other currents as well. Our results in the presence of CsCl could also have been explained, therefore, as (at least partial) effects on other ionic channels, reducing the impact of the previously suggested findings. To exclude this possibility, another channel blocker, known to be specific to the pacemaking current, was also tried. The effect of 10 μM ZD7288 is demonstrated in figure 6, where its effect on the spontaneous firing was tested first. Similar to the application of CsCl, ZD7288 effectively reduced the spontaneous firing to approximately 20% of the control value (fig. 6A, B), an effect very similar to that obtained in the presence of extracellular CsCl. Under voltage-clamp conditions (fig. 6C), ZD7288 reduced the amplitude of the hyperpolarization-activated current. Considering all the neurones tested with ZD7288 (n = 5), the blocking effect was very similar to that observed in the presence of 1 mM CsCl (fig. 6D and 4B). These experiments supported our view that the spontaneous firing of the pyramidal cells was mainly the consequence of the presence and activity of a pacemaker current identified as I_h.

As the majority of the experiments were conducted on relatively young animals, specific measurements were performed to see whether the current reported here was available on pyramidal cells of older (aged 18–23 days) rats. When these – more mature – nerve cells were subjected to hyperpolarizing stimuli, the activation of I_h was observed, indicating that this current was not only present at a relatively early stage of postnatal development, but also remained available in adult animals as well.

In the next step of the experiments, the possible subunit composition of the channels responsible for the genesis of the h-current was determined. For these experiments, acutely isolated pyramidal cells were employed, thus we looked for the presence of an h-type current in these neurones as well, to ensure that the enzyme treatment did not diminish these channel proteins. In all cases tested (n = 4), the presence of the h-type current could be demonstrated in freshly isolated pyramidal cells, and the

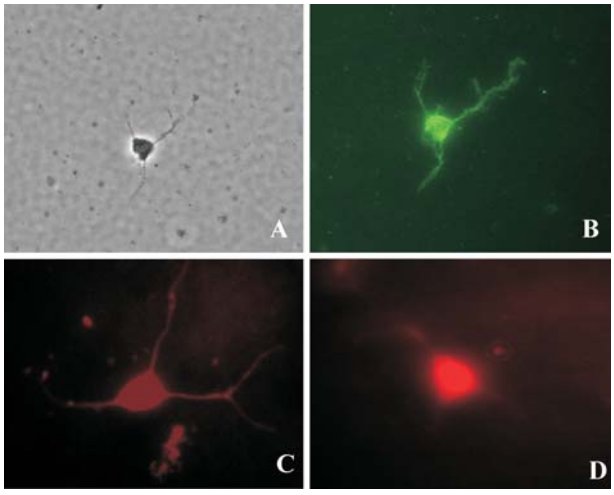

Figure 7. Immunocytochemical detection of HCN subunits. Images were taken with a Nikon Axiovert 600 microscope equipped with a × 200 objective. (*A*) Phase-contrast image of an acutely isolated pyramidal cell. (*B*) HCN2-specific immunoreaction (FITC) on the same neurone. (*C, D*) HCN1- and HCN4-specific (Texas Red) immunostainings, respectively with different neurons.

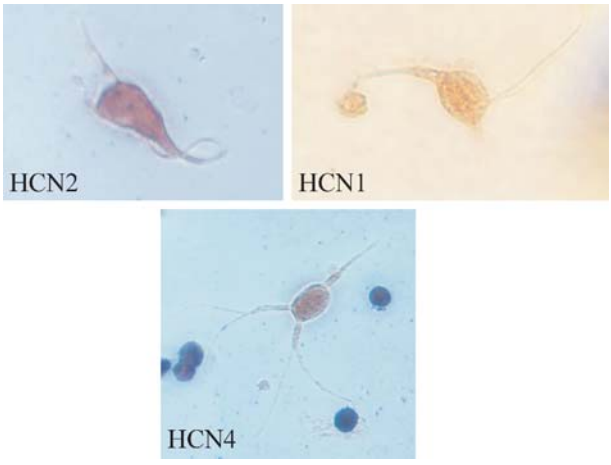

Figure 8. Immunolabelling of HCN1, HCN2 and HCN4 channel proteins in acutely isolated pyramidal cells using DAB-based visualization of the immunoreaction. The positive immunoreaction can be identified on the basis of the dark-brown colour seen on the cells.

major characteristic features of the current were identical to those found in pyramidal cells, situated in slices (data not shown). In these experiments, pyramidal cells were identified on the basis of the triangular cell body, and the multiple processes arising from the soma. The identity of the h-current was verified by the application of 1 mM CsCl as well as by the application of 10 µM ZD7288 (data not shown).

After confirming the presence of the I_h, immunocytochemical experiments were conducted to check whether the HCN subunits for which commercially available antibodies exist (HCN1, HCN2 and HCN4) contribute to the assembly of the functioning channels in the pyramidal cells of the dorsal cochlear nucleus. In these experiments, immunostaining was usually combined with DAPI labelling of the nuclei to demonstrate the integrity of the neurones. Figure 7A shows an isolated pyramidal cell under phase-contrast optics, while figure 7B demonstrates an HCN2-subunit-specific immunoreaction on the same neurone. Similar to the HCN2 subunits, a positive immunorection was found when anti-HCN1 and anti-HCN4 antibodies were tested (fig. 7C, D, respectively, different cells). Besides the application of the FITC- and Texas-Red-conjugated secondary antibodies, all immunoreactions were performed with DAB-conjugated antibodies as well (fig. 8). In the immunocytochemical experiments, every cell which was identified as a pyramidal neurone showed immunopositivity for all subunits tested. The specificity of the immunolabelling was confirmed in two ways. HCN-specific immunostaining was carried out on cochlear astrocytes maintained in tissue culture, and no positive immunolabelling could be observed in these experiments. This finding is in good agreement with our electrophysiological results showing no indication of h-current activation on these glial cells (unpublished observation). Moreover, the HCN-specific immunostaining was also performed using preadsorbed controls, giving only a very weak reaction.

Discussion

In this work, the presence of a hyperpolarization-activated current was demonstrated in the pyramidal cells of the dorsal cochlear nucleus. This current was the consequence of the activation of non-specific cationic channels, and the general properties of this current were very similar to the h-current reported on other neurones of the brain, including some nerve cells of the auditory pathway. Pyramidal cells had an intrinsic ability to fire action potentials, and the firing frequency was reduced to ~20% of the control if the h-current was inhibited, regardless of whether CsCl or the more specific ZD7288 was applied in the experimental solution. These experimental findings suggest that the presence and activity of the h-current provides a pacemaking ability for the pyramidal cells. However, this mechanism seems not to be the only factor contributing to the intrinsic firing of these neurones, as spontaneous action potentials could be recorded even after the practically complete inhibition of the h-current.

We have known for some time that some cells respond with an increased membrane conductance to hyperpolarization. Such a phenomenon was first described by Katz [19] in skeletal muscles, and this phenomenon is regarded as the ‘classical’ inward rectification. However, some tissues possess a different type of hyperpolarization-activated current (I_h), originally described in photoreceptors [20] and in the heart [12–14].

Our experimental findings indicate that the activation of the hyperpolarization activated channels expressed by the pyramidal cells of the dorsal cochlear nucleus produces an h-type current. First, the reversal potential of this current was approximately –33 mV, indicating that it represented a mixed cationic conductance, rather than a pure K^+ current. Similar values have been recorded in some other neurones, including the principal cells of the medial nucleus of the trapezoid body [21], hippocampal neurones [22] and neurones of the cat sensorimotor cortex [23].

Besides the reversal potential, the pharmacological sensitivity of the current also indicated that the current investigated in the present study was a non-specific conductance. In accordance with the data found in the literature [21, 24–26], the channels found here proved to be sensitive to Cs ions, as 1 mM CsCl had a blocking effectivity of ~85% at –140 mV. Moreover, they were also very effectively inhibited by ZD7228, a bradycardic agent known to be specific for the hyperpolarization-activated non-specific cationic current providing the pace-making ability of the sinu-atrial cells [27] and certain neurones [28].

Hitherto, four genes have been found to be responsible for encoding hyperpolarization-activated non-specific cationic channel subunits [29–34], and the four subunits (termed HCN1–HCN4) most likely form tetrameric channels in either homo- or heterotetrameric fashion. Individual subunits are understood to contain six putative transmembrane segments, and the HCN channels contain a cyclic nucleotide-binding domain as well. The activation time constant of HCN1-containing channels was found to be about 100 ms, while the HCN2-containing ones were slower, with an activation time constant of some 250 ms. HCN3 and HCN4 channels also produce slowly activating current (particularly the HCN4 subtype). In the light of these observations, the activation time constants reported in the present study (τ_1 = 150–400 ms, τ_2 = 800–1600 ms) suggested that the channels responsible for the genesis of the hyperpolarization-activated current of the pyramidal cells contained relatively slowly activating HCN subunits. This idea was in accordance with the findings of Santoro et al. [35], who demonstrated very strong expression of HCN2-specific mRNA along with the presence of mHCN1 at a moderate level as well as mHCN4 at a low level in the cochlear nucleus. Our electrophysiological and immunocytochemical results show that the appropriate genes are not only transcribed to mRNA but are actually translated to proteins which are expressed in the surface and form functional channels in the pyramidal cells. Although the methods used in this study cannot provide the exact subunit composition of the channels responsible for the genesis of the hyperpolarization-activated current of the pyramidal cells, those subunits for which commercially available antibodies exist are present, and are likely to contribute to the assembly of the functional channels.

The view that the hyperpolarization-activated channels of the pyramidal cells are unlikely to be HCN1 homotetramers is further emphasized by the fact that the activation time constants of the h-current obtained here were reasonably similar (τ_1: 420 versus 591 ms; τ_2: 1700 versus 4970 ms) to those obtained from recombinant HCN2 channels (at membrane potentials of –100 mV and –104 mV, respectively). Recombinant HCN1 channels, on the other hand, had much faster gating (τ_1 and τ_2: 79 and 339 ms, respectively). Quite interestingly, the activation time constants of the pyramidal h-current and the recombinant HCN2 channels are similar but not the same, suggesting that other subunits (for example HCN4) may also contribute to the final assembly of the channels.

One must note that the activation time constants found in the present study are very similar to those reported on thalamic relay neurones (364 and 2140 ms [16]). Thalamic relay neurones are also capable of producing spontaneous action potentials, and the hyperpolarization-activated current has a major contribution to this phenomenon.

Functional considerations

The expression of the hyperpolarization-activated cationic channels is remarkably widespread along the acoustic pathway, as the activity of these channels has been reported on inner hair cells, type I spiral ganglion neurones, bushy cells, principal cells of the medial nucleus of the trapezoid body and cells of the superior olive [21, 36–38]. The h-current is known to be involved in several different functions in other neurones, as it may set the resting membrane potential of the cells [39] and may also prevent long-lasting inhibition of the neurones [40]. Such a role seems to be possible in the cases of the pyramidal cells as well, since pyramidal cells are clearly contacted by inhibitory interneurones and the presence of inhibitory postsynaptic potentials and currents has also been demonstrated [7]. A particularly interesting function of the I_h is its involvement in the genesis of spontaneous activity of certain types of neurones [15, 16], such as thalamic relay neurones. Previous studies have shown that the inhibition of the h-current by Cs^+ reduced the frequency of the spontaneous activity in these neurones in certain cases (although it was also able to increase the frequency of the intrinsic firing). A similar function was noted on the pyramidal cells of the cochlear nucleus in this study, and this observation indicates that pyramidal cells are (at least partially) responsible for the intrinsic activity of the dorsal cochlear nucleus.

However, as the almost complete inhibition of the h-current did not abolish the intrinsic firing of the pyramidal cells, one must assume that other cells also contribute to the pacemaking activity of the dorsal cochlear nucleus. One possibility is that the activity of some synaptic inputs to the pyramidal cells may serve as another source of the

activity of the pyramidal cells, although detailed investigation of this possibility remains to be completed.

The suggestion has been made that HCN1 subunits are mainly found in large principal neurones showing rich dendritic arborization and possessing far-reaching axons. In these neurones, I_h would help in the propagation of dendritic inputs, which, in turn, would help the integration of the various incoming signals [35]. Pyramidal cells do possess an extensive dendritic tree and they are important output neurones of the dorsal cochlear nucleus, and they do seem to present HCN1 subunits along with HCN2 and HCN4 subunits. Such a combination of the various subunits is not unheard of, as HCN2 subunits were found on GABA-ergic inhibitory neurones as well as on thalamocortical relay neurones, where they are combined with HCN4 subunits. As the thalamocortical interneurones are also capable of producing spontaneous action potentials, similar to the pyramidal cells, the HCN2/HCN4 subunit composition may provide the pacemaking ability of these two cell types.

Acknowledgements. This work was supported by grants from the Hungarian Science Foundation (OTKA T-31824 and OTKA 13B0-0/19/TS01). The authors are indebted to Dr. C. Harasztosi for his valuable suggestions and to Mrs. I. Varga for her skilled technical assistance.

1 Osen K. K. (1969) Cytoarchitecture of the cochlear nuclei in the cat. J. Comp. Neurol. **136:** 453–484
2 Lorente de No R. (1981) The Primary Acoustic Nuclei, Raven, New York
3 Rhode W. S., Smith P. H. and Oertel D. (1983) Physiological response properties of cells labeled intracellularly with horseradish peroxidase in cat dorsal cochlear nucleus. J. Comp. Neurol. **213:** 426–447
4 Webster D. B. and Trune D. R. (1982) Cochlear nuclear complex of mice. Am. J. Anat. **163:** 103–130
5 Osen K. K. (1972) Projection of the cochlear nuclei on the inferior colliculus in the cat. J. Comp. Neurol. **144:** 355–372
6 Ryugo D. K., Willard F. H. and Fekete D. M. (1981) Differential afferent projections to the inferior colliculus from the cochlear nucleus in the albino mouse. Brain. Res. **210:** 342–349
7 Zhang S. and Oertel D. (1994) Neuronal circuits associated with the output of the dorsal cochlear nucleus through fusiform cells. J. Neurophysiol. **71:** 914–930
8 Pfeiffer R. R. (1966) Classification of response patterns of spike discharges for units in the cochlear nucleus: tone-burst stimulation. Exp. Brain Res. **1:** 220–235
9 Kanold P. O. and Manis P. B. (1999) Transient potassium currents regulate the discharge patterns of dorsal cochlear pyramidal cells. J. Neurosci. **19:** 2195–2208
10 Hirsch J. A. and Oertel D. (1988) Intrinsic properties of neurones in the dorsal cochlear nucleus of mice, in vitro. J. Physiol. **396:** 535–548
11 Harasztosi C., Forsythe I. D., Szûcs G., Stanfield P. R. and Rusznák Z. (1999) Possible modulatory role of voltage-activated Ca^{2+} currents determining the membrane properties of isolated pyramidal neurones of the rat dorsal cochlear nucleus. Brain Res. **839:** 109–119
12 Brown H., DiFrancesco D and Noble S. (1979) Cardiac pacemaker oscillation and its modulation by autonomic transmitters. J. Exp. Biol. **81:** 175–204
13 Brown H. A. and DiFrancesco D. (1980) Voltage clamp investigations of currents underlying pacemaker activity in rabbit sino-atrial node. J. Physiol. **308:** 331–351
14 DiFrancesco D. (1993) Pacemaker mechanisms in cardiac tissue. Annu. Rev. Physiol. **55:** 455–472.
15 Bal T. and McCormick D. A. (1997) Synchronized oscillations in the inferior olive are controlled by the hyperpolarization-activated cation current I_h. J Neurophysiol. **77:** 3145–3156
16 McCormick D. A. and Pape H. C. (1990) Properties of a hyperpolarization-activated cation current and its role in rhythmic oscillation in thalamic relay neurones. J. Physiol. **431:** 291–318
17 Rusznák Z., Forsythe I. D., Brew H. M. and Stanfield P. R. (1997) Membrane currents influencing action potential latency in granule neurons of the rat cochlear nucleus. Eur. J. Neurosci. **9:** 2348–2358
18 Rusznák Z., Harasztosi C., Stanfield P. R. and Szûcs G. (2001) An improved cell isolation technique for studying intracellular Ca^{2+} homeostasis in neurones of the cochlear nucleus. Brain Res. Prot. **1:** 68–75
19 Katz B. (1949) Les constants électriques de la membrane du muscle. Arch. Sci. Physiol. **2:** 285–299
20 Attwell D. and Wilson M. (1980) Behaviour of the rod network in the tiger salamander retina mediated by membrane properties of individual rods. J. Physiol. **309:** 287–315
21 Banks M. I., Pearce R. A. and Smith P. H. (1993) Hyperpolarization-activated cation current (I_h) in neurons of the medial nucleus of the trapezoid body: voltage-clamp analysis and enhancement by norepinephrine and cAMP suggest a modulatory mechanism in the auditory brain stem. J. Neurophysiol. **70:** 1420–1432
22 Halliwell J. V. and Adams P. R. (1982) Voltage-clamp analysis of muscarinic excitation in hippocampal neurons. Brain Res. **250:** 71–92
23 Spain W. J., Schwindt P. C. and Crill W. E. (1987) Anomalous rectification in neurons from cat sensorimotor cortex in vitro. J. Neurophysiol. **57:** 1555–1576
24 Schlichter R., Bader C. R. and Bernheim L. (1991) Development of anomalous rectification (I_h) and of a tetrodotoxin-resistant sodium current in embryonic quail neurones. J. Physiol. **442:** 127–145
25 Bader C. R., Bertrand D. and Schwartz E. A. (1982) Voltage-activated and calcium-activated currents studied in solitary rod inner segments from the salamander retina. J. Physiol. **331:** 253–284
26 Mayer M. L. and Westbrook G. L. (1983) A voltage-clamp analysis of inward (anomalous) rectification in mouse spinal sensory ganglion neurones. J. Physiol. **364:** 217–239
27 BoSmith R. E., Briggs I. and Sturgess N. C. (1993) Inhibitory actions of ZENECA ZD7288 on whole-cell hyperpolarization activated inward current (I_f) in guinea-pig dissociated sinoatrial node cells. Br. J. Pharmacol. **110:** 343–349
28 Harris N. C. and Constanti A. (1995) Mechanism of block by ZD7288 of the hyperpolarization-activated inward rectifying current in guinea-pig substantia nigra neurons in vitro. J. Neurophysiol. **74:** 2366–2378
29 Santoro B., Liu D. T., Yao H., Bartsch D., Kandel E. R., Siegelbaum S. A. et al. (1998) Identification of a gene encoding a hyperpolarization-activated pacemaker channel of brain. Cell **93:** 717–729
30 Santoro B., Grant S. G., Bartsch D. and Kandel E. R. (1997) Interactive cloning with the SH3 domain of N-src identifies a new brain specific ion channel protein, with homology to eag and cyclic nucleotide-gated channels. Proc. Natl. Acad. Sci. USA **94:** 14815–14820
31 Ludwig A., Zong X., Jeglitsch M., Hofmann F. and Biel M. (1998) A family of hyperpolarization-activated mammalian cation channels. Nature **393:** 587–591
32 Ludwig A., Zong X., Stieber J., Hullin R., Hofmann F. and Biel M. (1999) Two pacemaker channels from human heart with profoundly different activation kinetics. EMBO J. **18:** 2323–2329

33 Ishii T. M., Takano M., Xie L. H., Noma A. and Ohmori H. (1999) Molecular characterization of the hyperpolarization-activated cation channel in rabbit heart sinoatrial node. J. Biol. Chem. **274:** 12835–12839
34 Seifert R., Scholten A., Gauss R., Mincheva A., Lichter P. and Kaupp U. B. (1999) Molecular characterization of a slowly gating human hyperpolarization-activated channel predominantly expressed in thalamus, heart, and testis. Proc. Natl. Acad. Sci. USA **96:** 9391–9396
35 Santoro B., Chen S., Luthi A., Pavlidis P., Shumyatsky G. P., Tibbs G. R. et al. (2000) Molecular and functional heterogeneity of hyperpolarization-activated pacemaker channels in the mouse CNS. J. Neurosci. **20:** 5264–5275
36 Golding N. L., Ferragamo M. J. and Oertel D. (1999) Role of intrinsic conductances underlying responses to transients in octopus cells of the cochlear nucleus. J. Neurosci. **19:** 2897– 2905
37 Bal R. and Oertel D. (2000) Hyperpolarization-activated, mixed-cation current (I_h) in octopus cells of the mammalian cochlear nucleus. J. Neurophysiol. **84:** 806–817
38 Cuttle M. F., Rusznák Z., Wong A. Y., Owens S. and Forsythe I. D. (2001) Modulation of a presynaptic hyperpolarization-activated cationic current (I_h) at an excitatory synaptic terminal in the rat auditory brainstem. J. Physiol. **534:** 733–744
39 Maccaferri G., Mangoni M., Lazzari A. and DiFrancesco D. (1993) Properties of the hyperpolarization-activated current in rat hippocampal CA1 pyramidal cells. J. Neurophysiol. **69:** 2129–2136
40 Luo M. and Perkel D. J. (1999) A GABAergic, strongly inhibitory projection to a thalamic nucleus in the zebra finch song system. J. Neurosci. **19:** 6700–6711